Hot Jupiter Transit Observations

Ethan Lee and Necdet Canim, Contributor
(Dated: December 17, 2022)

Here we describe the process of observing transiting Hot Jupiter exoplanets from the Table Mountain Observatory telescope. We produced light curves for 3 different exoplanets, each with some interesting aspect of it which is very useful and is conducive to learning. Comparing our values to online databases, the drops in magnitude for each exoplanet transit remains consistent with others' findings.

I. INTRODUCTION

The study of exoplanets, or planets outside of our solar system, has yielded numerous discoveries in recent years, thanks in part to advances in technology that allow us to detect and analyze these distant worlds. One such class of exoplanet that has garnered significant interest is the hot Jupiter, a type of gas giant planet similar in size to Jupiter but with a much closer orbit to its host star. While planets this large often do not form in close orbit to its star, we believe they exist due to the planetary migration theory – one that says that these large gas giants likely migrated inwards upon formation. These close orbits result in high surface temperatures, making hot Jupiters some of the hottest known exoplanets. Despite their extreme temperatures, hot Jupiters are of great interest to astronomers due to their large size and ability to produce detectable transit events.

Transit photometry is a technique used to measure the properties of exoplanets, including their size and orbit. This method involves observing the small dip in brightness that occurs when a planet passes in front of its host star from the perspective of the observer, as can be seen in Figure 1. By analyzing the duration and depth of this transit, as well as the regularity of the transit events, astronomers can infer the size and orbit of the exoplanet.

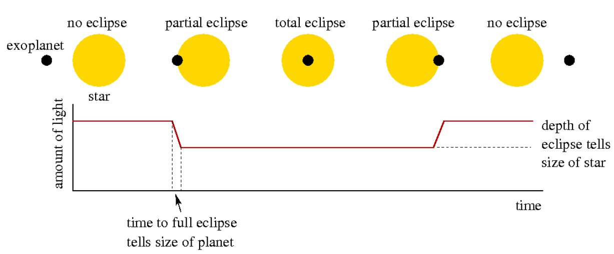

FIG. 1. When a planet passes in front of a star, it blocks some amount of the light for the duration of its transit. If one tracks how the brightness changes, one can find the ratio of the size of the planet and the host star $(R_p/R_{star})^2$.

In this lab report, we will use transit photometry to discuss the observation and analysis of three hot Jupiter transits: Qatar-1 b, WASP-52 b, and HAT-P-32 b. While in the past, we had looked at exoplanet transits through AstroImageJ, performing our transit photometry showed to yield interesting results. We will also discuss the potential implications of our findings and potential avenues for further research.

II. RELATED WORK

Exoplanet transits have been extensively studied in recent years, with many different methods and techniques developed to detect and characterize these events. Many efforts focused on using photometric observations to identify the periodic dips in brightness caused by transiting exoplanets – most of which make use of the large dip created by Hot Jupiters. For example, in this paper by Hellier et al [1], we can visualize the importance of Hot Jupiters in exoplanet transit photometry, stating that they are easy targets to study. This is because they produce deep transits as much as almost 1 percent and that they have short periods between 1 and 10 days. A similar understanding can be shown in this paper by Bean et al [2], they chose three Hot Jupiters as primary nominal targets (WASP-79b, WASP-43b, WASP-18b) for The Transiting Exoplanet Community Early Release Science Program for JWST. They chose these planets under the sentiment that they produce much more obvious light curves and can easily be observed over multiple nights.

We can also see how effective our targets are for learning in a student paper by Dhiraj Bansal, Dana Cody, Chloe Herrera at Baylor University [3]. They make use of one of our targets, Qatar-1 b to demonstrate the phenomenon known as limb darkening, which shows that the center of a star appears brigher than its edges. They observed the hot Jupiter, Qatar-1b, using differential photometry to generate a light curve of the transit. Physical characteristics of the exoplanet were found in the paper by fitting a limb-darkened, light curve equation to the collected data. While we do not possess the tools to fit a limb-darkened light curve to the data, we can still perform this same experiment on our own telescope to yield interesting results.

III. OBSERVATION

As seen in Figures 2 and 3, the sky is pretty quiet and we are therefore set to observe – the moon is out of the way and there are no limiting factors that could be potentially dangerous to the telescope. For this observation, I collaborated with Necdet Canim to take observation data. We pulled finding charts from the Variable Star and Exoplanet Section of the Czech Astronomical Society's database to find our given stars. With these, we were able to locate and track our stars in the sky.

	DESCRIPTION	Moon	TEMP	PRECIP	HUMIDITY	WIND (mph)
Weather Notes:	CLEAR	72%	37.9F	0%	47%	3
Observing Plan	Wasp-52 b					

FIG. 2. Weather Summary for 11.14.22

	DESCRIPTION	Moon	TEMP	PRECIP	HUMIDITY	WIND (mph)
Weather Notes:	CLEAR	56%	33.2F	0%	20%	3
Observing Plan	Qatar-1b, HAT-P32 b					

FIG. 3. Weather Summary for 11.16.22

Based on the magnitudes of our targets (around 12), it made sense to observe with 10-second exposure times on the g or r filters. As can be seen in Figures 4 and 5, there were no failures in observation.

While doing our observations, we also set up the Unistellar eVscope telescope. Our goal in setting this telescope up was to make observations with the telescope and make comparisons between that and our TMO telescope.

However, we were not able to get good data out of the Unistellar telescope due to different data-taking methods. One of our observations (of Qatar-1 b) began right after sunset, so some light still lingered in the atmosphere. However, as we will see later, this proved to be a non-issue.

Target Name	Local Time	Sidereal Time	RA	Dec	Exp Time	Filter	Sky Brightness	ERRORS	Comments
wasp-52b	18:48	22 34 36	23 14 03	08 50 37.4	10s x 450	g			started collecting the first half of data (450 x 10 s exposures) name=wasp_1 focus=48100
wasp-52b	19:10	22 56 50	23 14 03	08 50 37.4			19.88		checked if there is a tracking failure: no failure
wasp-52b	19:24	23 10 12	23 14 03	08 50 37.0					checked if there is a tracking failure: no failure
wasp-52b	19:38	23 24 34	23 14 03	08 50 37.0					checked if there is a tracking failure: no failure
wasp-52b	19:52	23 38 30	23 14 03	08 50 37.0					checked if there is a tracking failure: no failure
wasp-52b	8:08 PM	23 55 06	23 14 01	08 51 22	10s x 450	g	19.91		started collecting the second half of the data (450 x 10 s exposures) name = wasp_2
wasp-52b	8:27 PM	00 13 56	23 14 01	08 51 23.2					defocused to 47900
wasp-52b	8:35 PM	00 21 56	23 14 01	08 51 22.9					checked if there is a tracking failure: no failure
wasp-52b	9:00 PM	00 46 44	23 14 01	08 51 23.2					checked if there is a tracking failure: no failure
wasp-52b	9:11 PM	00 57 51	23 14 01	08 51 23.0					checked if there is a tracking failure: no failure. Also, temperature is 34.14F, approaching 32F
wasp-52b	9:22 PM	01 08 21	23 14 01	08 51 23.0					checked if there is a tracking failure: no failure. Also, temperature is 33.78F
wasp-52b	9:24 PM	01 10 33	23 14 01	08 51 23.0			19.88		completed collecting data

FIG. 4. Observation Summary for 11.14.22

Target Name	Local Time	Sidereal Time	RA	Dec	Exp Time	Filter	Sky Brightness	ERRORS	Comments
qatar 1-b	17:44	21:37:24	20 13 33.9	65 01 53.7	450 x 10s	r	18.45		started collecting the first half of data focus=47900
qatar 1-b	18:00	21:53:42	20 13 33.9	65 01 53.7					checked if there is a tracking failure: no failure
qatar 1-b	18:11	22:05:20	20 13 33.9	65 01 53.6					checked if there is a tracking failure: no failure
qatar 1-b	18:24	22:18:30	20 13 34.0	65 01 53.9					checked if there is a tracking failure: no failure. Also, there is 3,1m/s wind and 30% humidity
qatar 1-b	18:45	22:39:23	20 13 34 0	65 01 53.7					checked if there is a tracking failure: no failure.
qatar 1-b	7:02 PM	22:55:50	20 13 30	65 03 49.4	200 x 10s	r	20.45		started collecting the second half of data, focus=47900, also recentered
qatar 1-b	7:18 PM	23 12 44	20 13 30	65 03 49.6					checked if there is a tracking failure: no failure.
qatar 1-b	7:35 PM	23 29 14	20 13 30	65 03 50					completed taking data
hat-p-32b	21.41	01 35 57	02 04 17.5	46 40 02.6	360 x 10s	r	19.99		started taking the first of three datasets (first hour)
hat-p-32b	22.06	02 01 02	02 04 17.5	46 40 02.6					checked if there is a tracking failure: no failure.
hat-p-32b	10:27 PM	02 21 32	02 04 17.5	46 40 03.1					checked if there is a tracking failure: no failure.
hat-p-32b	22.44	02 39 20	02 04 15.2	46 41 09.9	360 x 10s	r	19.93		recentered and started taking the second of three datasets (second hour)
hat-p-32b	11:31 PM	03 25 37	02 04 15.2	46 41 09.8					checked if there is a tracking failure: no failure.
hat-p-32b	11:47 AM	03 42 06	02 04 12.7	46 41 45.4	600 x 10s	r	19.95		recentered and started taking the third (last) dataset

FIG. 5. Observation Summary for 11.16.22

Once we have observed and obtained our data, we can not do an analysis on it yet. We first must reduce our images as to increase our Signal-to-Noise Ratio (SNR) on all of our images. This allows for a more robust photometry calculation, as the sky brightness dims relative to the brightness to our stars, allowing our images to more easily be read by a computer. To achieve this, we subtracted darks, biases, and flats from each of our images. Darks and Biases are used to remove any 'cold' or 'hot' pixels, while flats are used to eliminate vignetting/light falloff.

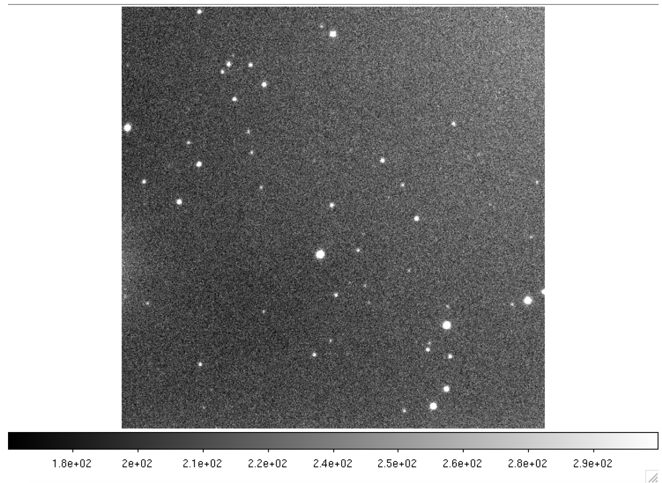

FIG. 6. Unfiltered 6' by 6' image of Qatar-1. Taken in the r filter on November 17, 2022 at 1:44 UTC. There is a lot of noise in the background which can easily confuse a computer which wishes to perform photometry. The scale at the bottom shows how the color corresponds to how many photons are hitting that pixel; white areas represent stars (which emit more photons per second) whereas darker areas have less photons.

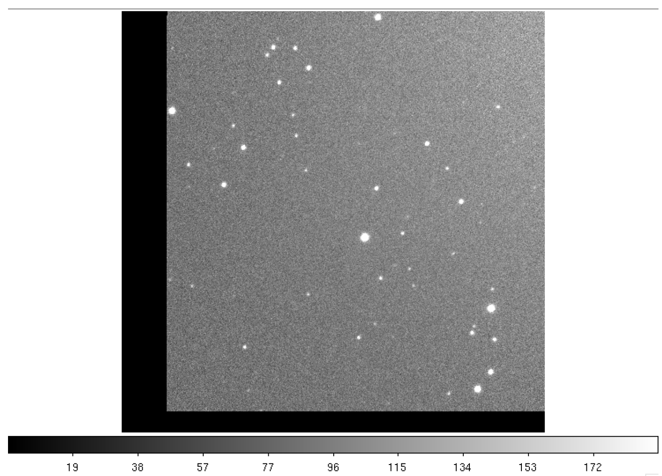

FIG. 7. Flats Darks and Biases reduced 6' by 6' image of Qatar-1. Taken in the r filter on November 17, 2022 at 1:44 UTC. Compared to Figure 6, the background is less noisy and more consistent, and therefore it is easier to perform photometry on these images. This image is aligned to a reference image, so the black L in the bottom right is empty space/is not the image. The scale at the bottom shows how the color corresponds to how many photons are hitting that pixel; white areas represent stars (which emit more photons per second) whereas darker areas have less photons.

Looking at Figures 6 and 7, we can see that our reduced image is much clearer, making photometry less difficult for the computer programs. To get a clear image of the night, we aligned the many exposures we took, as can be seen in Figure 8.

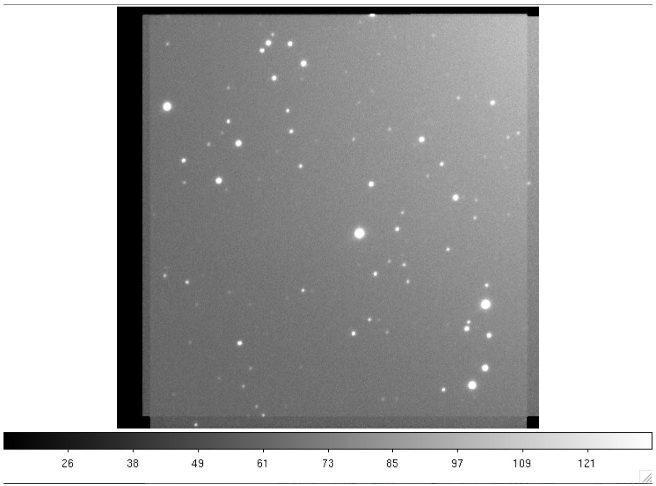

FIG. 8. Combined and aligned 6' by 6' image of Qatar-1 under the r filter. This image is aligned to a reference image, so the black L in the bottom right is empty space/is not the image. The scale at the bottom shows how the color corresponds to how many photons are hitting that pixel; white areas represent stars (which emit more photons per second) whereas darker areas have less photons.

IV. ANALYSIS

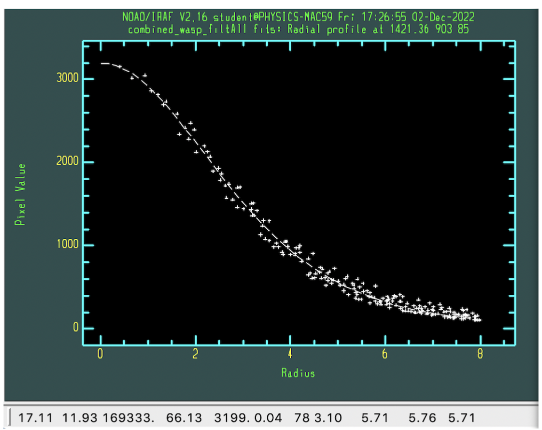

FIG. 9. Graph of photon drop-off of star WASP-52. Y-axis is the number of photons per pixel, and the x-axis is the number of pixels away from the center of the star. We can use this to calculate FWHM; the largest drop off can be approximated to the 2.8 pixels radius mark. Therefore, the FWHM should be around 5.6. Luckily, the computer calculates this for us using three different methods; these three calculations are the last three numbers on the bottom bar. Therefore, we can use a calculated FWHM of 5.71.

In order to do any calculations, we must first know the full width at half maximum (FWHM) of our stars. Looking at where our light is falling off at the largest rate in Figure 9, we know that the FWHM of WASP-52 to be roughly 5.73 $\pm$0.03. We will use this value, along with photoutils's DAOStarFinder (which performs source detection), to perform photometry on our data.

Now that we have our FWHM, we can perform photometry on our stars! For the purposes of this paper, I will not show our raw light curves since they are not particularly useful compared to the differential light curves. However, just looking at our differential light curves also does not tell us much as can be seen in Figure 10.

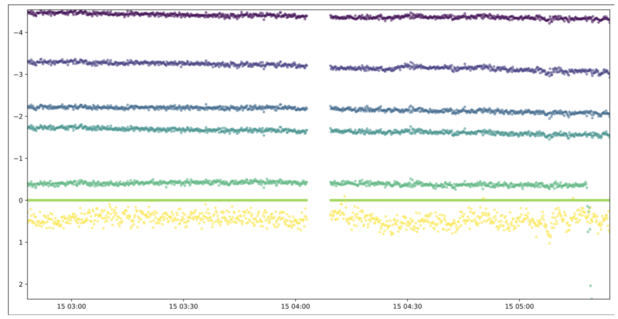

FIG. 10. Example differential light curve. Y-axis is of the difference in magnitude from the reference star (light green), which sits at a y-value of 0. X-axis is of the time in UT. There are not too many takeaways from the graph, as the dark purple plot (WASP-52) does not seem to change much.

Looking at the figure, there is not much to take away. This is because our dip in magnitude is around 0.02, so it is such a small dip that we can't see it so zoomed out. However, if we zoom in on our target, we can see that there is a dip in magnitude such as in Figure 11:

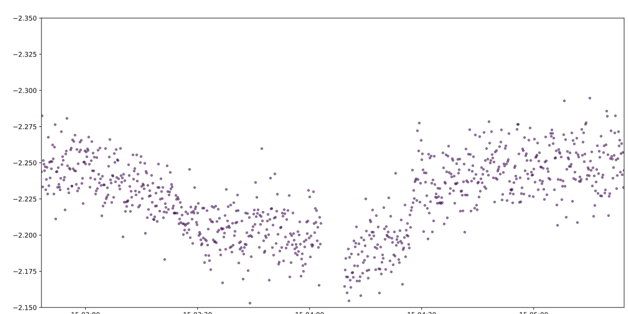

FIG. 11. Zoomed in differential light curve of the exoplanet transit of WASP-52 b using aperture size 2 pixels. Using the third brightest star in the frame as reference, we measured a 0.04 $\pm$0.038 mag drop. This corresponds well to the true dv=0.029. Y-axis corresponds to differential magnitude and the x-axis corresponds to the time.

By using geometry, we can estimate that, assuming a roughly spherical planet and star, the drop in magnitude is equivalent to the radius of the planet squared over the radius of the star squared. So, using WASP-52 b as an example, we can find the radius of the planet using the radius of the star:

$$\begin{aligned}
dv &= 0.029 \\
0.029 &= \frac{R_{planet}^2}{R_{star}^2} \\
R_{star} &= 0.79 R_{sun} \\
R_{planet}^2 &= 0.79^2 * 0.029 \\
R_{planet} &= 0.134 R_{sun} \\
R_{planet} &= 1.31 R_{Jupiter}
\end{aligned}$$

The real value is 1.27 $R_{Juputer}$; our calculations yield roughly the same results. We can perform similar calculations on Qatar-1 b and HAT-P-32 b, as they also produce similar light curves as shown in Figures 12 and 13.

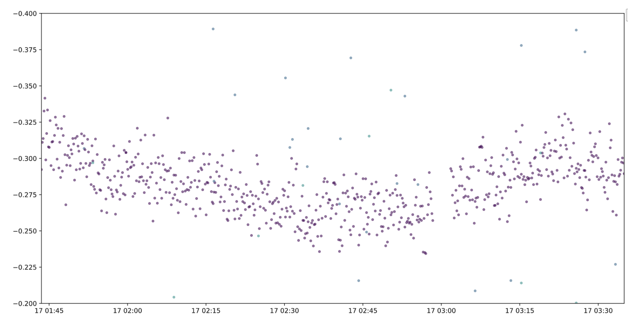

FIG. 12. Zoomed in differential light curve of the exoplanet transit of Qatar-1 b using aperture size 2 pixels. Using the second brightest star in the frame as reference, we measured a 0.025 ±0.02 mag drop. This corresponds well to the true dv=0.0204. Y-axis corresponds to differential magnitude and the x-axis corresponds to the time.

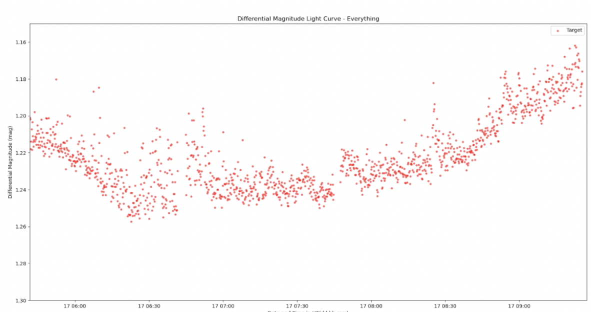

FIG. 13. Zoomed in differential light curve of the exoplanet transit of HAT-P-32 b using aperture size 4 pixels. Using the brightest star in the frame as reference, we measured a 0.03 ±0.01 mag drop. This corresponds well to the true dv=0.0244. Y-axis corresponds to differential magnitude and the x-axis corresponds to the time.

As you may notice, all three light curves do not form perfect trapezoidal drops, which leads to interesing discussion.

V. DISCUSSION

One obvious distinction between the curves is the smoothness of the light curve for Qatar-1 b (Figure 12. One odd solution to this smoothness could be the potential of the planet transiting the top of the visible sphere of the star Qatar-1, but this is not the case. Qatar-1 is a strong example of limb darkening. As was seen in the Baylor paper from earlier[3], limb darkening causes the light curve to smooth out due to the outsides of the visible disk of Qatar-1 appearing less bright than the center.

Another interesting result from these light curves can be seen in Figure 11. There appears to be a gap in the middle of the plot, in which there appears to have been some sort of dip in brightness. First, let us discuss why there is a break in all of the light curves.

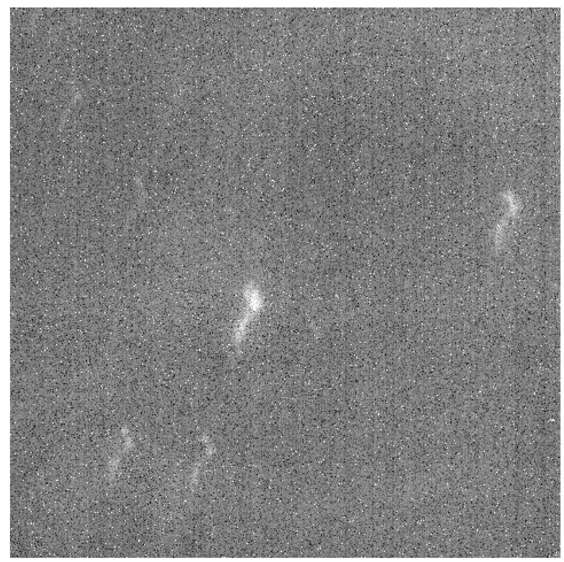

FIG. 14. Unaligned combined image of the first image cube of star WASP-52. This image follows a similar scale to those in Figures 6 and 8. Taken in the g filter on November 15, 2022. As can be seen, the star is moving in our frame of view throughout the night.

Throughout the night, our telescope up at Table Mountain Observatory tracks the location of our stars through the night sky. However, our telescope experiences a slight drift when taking data as can be seen in Figure 14; there is potential that our target star might fall out of frame. Therefore, we reset in the middle of observation to realign our telescope to our target star.

However, this does not explain why Figure 11 experiences a dip in brightness during this reset. This dip in brightness has nothing to do with the actual star itself nor its exoplanet transit, but rather it is likely due to how we reduced our images. While reducing darks and biases have small effects to the brightness of our targets, reducing flats can have an effect which is apparent here.

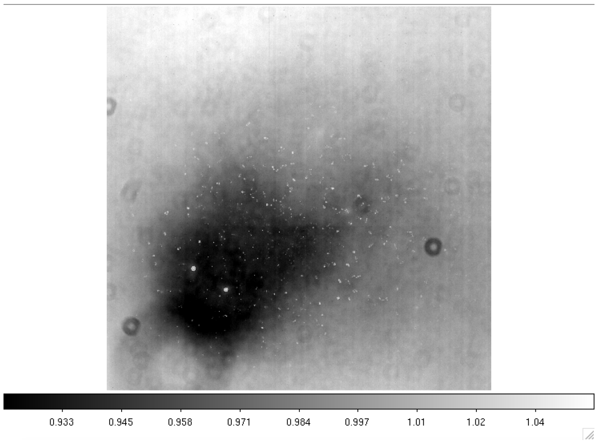

FIG. 15. Flat fielding in the g-band. These are adjustments that are made to the brightness at each pixel based on how the TMO telescope sees brightness in the frame. On this scale, brighter white means that more is subtracted from these pixels, whereas darker pixels will subtract less.

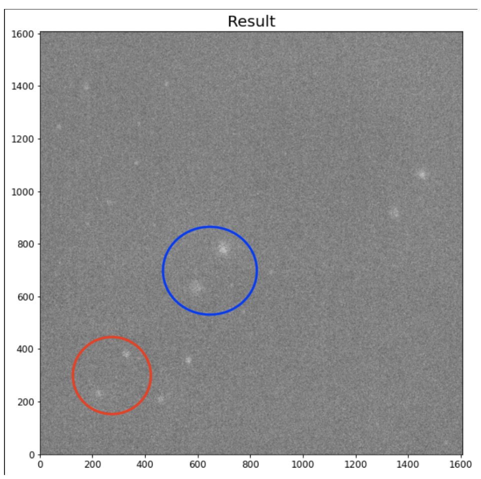

FIG. 16. Combined image of the first and last frame of the first image cube of WASP-52. The points circled in red represent the reference star used, while the blue represents the target star. Images taken in the g filter; x and y axes represent pixel values. As can be seen, throughout the observation the star drifts up the x and y axes.

Taking a look at Figure 15, we can see that one area of the telescope's field of view in the bottom left is altered significantly differently than the rest. This is likely because there is something wrong with the lens or such which needs generally be corrected. However, I believe that this mark can have small effects our light curve. Looking at Figure 16, we can see our stars (in our frame of view) moving in the positive x and y directions. While this does not seem too conspicuous, looking back at our flat fielding in Figure 15, it appears that our reference star (in red) has move from away from the "dark" zone into that zone while our target star (in blue) has moved out of that zone. In the small break in Figure 11, we moved our stars back to the original bottom right positions. Thanks to our flat fielding corrections, our reference star will be corrected to be a little brighter and our target star to be less bright. Because of this, I believe that when realigning our telescope our brightness changed ever so slightly.

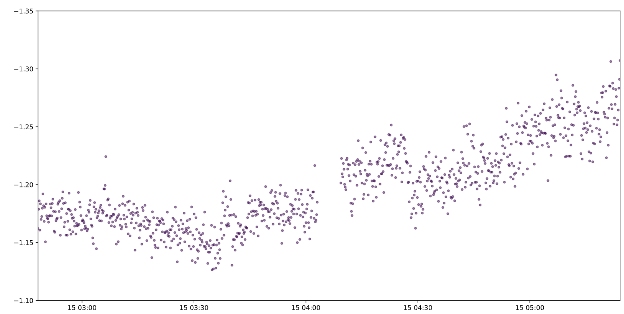

FIG. 17. Zoomed in differential light curve of the exoplanet transit of WASP-52 b using aperture size 2 pixels. Using the second brightest star in the frame as reference, we can not measure a drop in brightness due to the upward trend on the brightness. Y-axis corresponds to differential magnitude and the x-axis corresponds to the time.

Another interesting point that brought a good amount of struggle was the choosing of reference stars. For example, when I first produced a light curve for WASP-52, The light curve (as can be seen in Figure 17, produced an upward trend. At first glance, it is easy to assume that there was likely an error when producing this light curve. However, at times such as 15 3:40 and 15 4:30, there are very obviously large shifts in brightness suggesting that there is some sort of movement happening.

However, we were still able to produce a good light curve for the target in Figure 11, why is that? This is due to an anomaly of a reference star. In our upward trending graph, we used the second brightest star as reference, as brighter reference stars can give more accurate results. However, after seeing the third and fourth brightest reference stars producing decent light curves, it is obvious that the second brightest star in the frame was likely experiencing a pulsating brightness due to some unknown factor.

One trend that I have yet to address until now is the slight upward trend of the transit of HAT-P-32 b (Figure 13). When seeing this, I followed the same sentiment as the previous paragraph, searching various reference stars to find a reference star which created a solid differential light curve. However, most reference stars were not producing nice light curves similar to the first two objects. All of the reference stars were producing light curves with some sort of trend upwards or downwards. In Figure 18, we can see a slight downwards trend on our overall messy light curve.

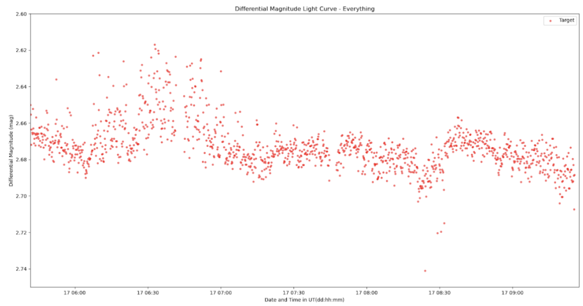

FIG. 18. Zoomed in differential light curve of the exoplanet transit of HAT-P-32 b using aperture size 4 pixels. Using the fifth brightest star in the frame as reference, we can see a drop in brightness with oddities. Y-axis corresponds to differential magnitude and the x-axis corresponds to the time.

Rather than simply guessing and checking these reference stars, we can look at plots of our reference stars to see which ones are not going to be useful. For example, in the differential light curve in Figure 19, we use a star not in frame as a reference, and the rest of the reference stars are shown in frame. As you can see, the light curves all seem to follow a similar trend, suggesting that their brightness is static relative to one another. So, these reference stars should be useful.

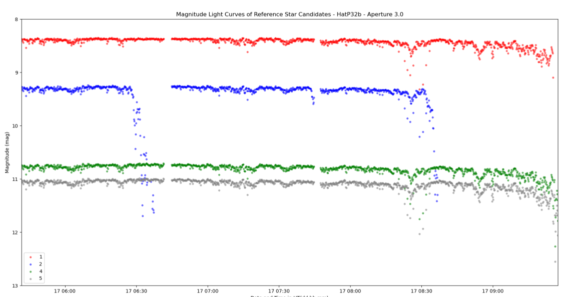

FIG. 19. Zoomed in differential light curve of our reference stars for HAT-P-32 b. As we can tell, all of the reference star candidates in the frame follow the same trend, suggesting that all of the light curves are likely viable to use as reference stars. These light curves seem to experience dips and such, so it is likely that the reference star used here is not ideal to be used as a reference. Y-axis corresponds to differential magnitude and the x-axis corresponds to the time.

For more on reference stars, refer to the similar paper written by Necdet Canim.

Our light curves also seem to have extremely broad ranges of brightness; for example our Figure 11 has an error range of ± 0.038. In exoplanetary transits, this is a huge margin for error. In order to cut down on this error, we can perform binning on our data, which averages the brightness data from each minute rather than plotting all ten second exposures. In Figure 20, we can see that the attempted binning did not thin out the data, but rather made the data more sparse. However, again, this data does not change much as can also be seen in Necdet Canim's paper.

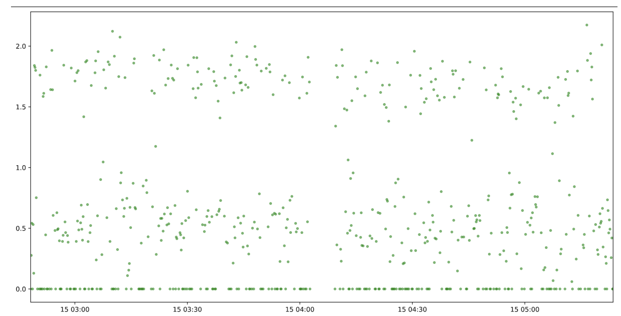

FIG. 20. Differential light curve plot of binned data of WASP-52 b. As can be seen, the data is more sparse and did not contract into a smaller, easier light curve to measure. The top blurb of data is WASP-52, while the second is the second brightest star in the frame. At the bottom is the third brightest star in frame, which is used as reference. Y-axis corresponds to differential magnitude and the x-axis corresponds to the time.

Initially, the project's goal was to look at any differences in how the Unistellar telescope can deal with exoplanet transits – will it see the same turbulence in the sky? How would these light curves compare? However, working with this data proved to be too difficult, as each .fits image came similar to the image provided in Figure 21:

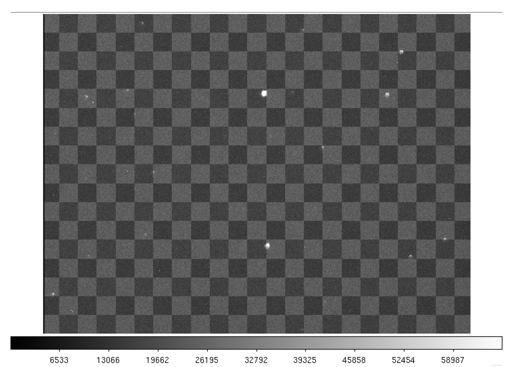

FIG. 21. Image taken using the Unistellar telescope of WASP-52. This image .fits data is unfamiliar to us, so the aperture photometry would be much more difficult than intended.

VI. CONCLUSIONS

While we were not able to use aperture photometry on our Unistellar data, we were still able to take observations with the TMO telescope and extract lots of interesting learnings. A special thanks is extended to Professor Phillip Choi and Nez Evans for guiding us through the observation process. Looking forwards, it would be very interesting to produce zoomed in reference star plots along with our data, so that we can look at our data while also looking at our reference stars. We could also calculate the strength of limb darkening for each planet, similar to the paper on Qatar-1 at Baylor University [3]. It will be imperative in the future to look into different forms of binning, as the current methods used were largely ineffective and still produce shaky results. Using these more precise numbers, we would potentially be able to use S. Seager and G. Mallén-Ornelas's equations [4] to provide much more data about our transiting exoplanet. Lastly, working with the Unistellar data could provide for interesting observations on the night sky and also on light curve data for the night. With all of this in mind, there is surely more work to be done.

---

[1] Hellier, C., Anderson, D. R., Bouchy, F., Burdanov, A., Cameron, A. C., Delrez, L., Gillon, M., Jehin, E., Lendl, M., Nielsen, L. D., Maxted, P. F., Pepe, F., Pollacco, D., Queloz, D., Ségransan, D., Smalley, B., Triaud, A. H., Udry, S., & West, R. G. (2018). New transiting hot Jupiters discovered by WASP-south, Euler/Coralie, and TRAPPIST-South. Monthly Notices of the Royal Astronomical Society, 482(1), 1379–1391.

[2] Bean, J. L., Stevenson, K. B., Batalha, N. M., Berta-Thompson, Z., Kreidberg, L., Crouzet, N., Benneke, B., Line, M. R., Sing, D. K., Wakeford, H. R., Knutson, H. A., Kempton, E. M.-R., Désert, J.-M., Crossfield, I., Batalha, N. E., Wit, J. de, Parmentier, V., Harrington, J., Moses, J. I., . . . Zingales, T. (2018). The Transiting Exoplanet Community early release science program for jwst. Publications of the Astronomical Society of the Pacific, 130(993), 114402. `https://doi.org/10.1088/1538-3873/aadbf3`

[3] Light Curve Analysis for Transit of Exoplanet Qatar-1b by Dhiraj Bansal, Dana Cody, Chloe Herrera, Dr. Dwight Russell, and Mr. Richard Campbell at Baylor University

[4] S. Seager and G. Mallén-Ornelas 2003 ApJ 585 1038 `https://doi.org/10.1086/346105`